

Size-dependent optimal microstructure design based on couple-stress theory

Wenzheng Su · Shutian Liu

Received: 16 May 2009 / Revised: 25 December 2009 / Accepted: 8 January 2010 / Published online: 5 February 2010
© Springer-Verlag 2010

Abstract The purpose of this paper is to propose a size-dependent topology optimization formulation of periodic cellular material microstructures, based on the effective couple-stress continuum model. The present formulation consists of finding the optimal layout of material that minimizes the mean compliance of the macrostructure subject to the constraint of permitted material volume fraction. We determine the effective macroscopic couple-stress constitutive constants by analyzing a unit cell with specified boundary conditions with the representative volume element (RVE) method, based on equivalence of strain energy. The computational model is established by the finite element (FE) method, and the design density and FE stiffness of the RVE are related by the solid isotropic material with penalization power (SIMP) law. The required sensitivity formulation for gradient-based optimization algorithm is also derived. Numerical examples demonstrate that this present formulation can express the size effect during the optimization procedure and provide precise topologies without increase in computational cost.

Keywords Couple-stress · Size effect · Topology optimization · RVE · Cellular materials

1 Introduction

An interesting feature of structural optimization is that the optimal solution to the problem involves microstructures in certain cases. The purpose of the topology optimization technique is to propose an approach of fulfilling the efficient layout of limited material in the design of different settings (Bendsøe and Kikuchi 1988; Bendsøe 1989; Bendsøe and Sigmund 2004). For optimization purpose it is usually sufficient to consider only composites with periodic microstructures. And for composite with periodic microstructures, its effective properties may be fully described by an analysis of the smallest repetitive unit, i.e. the base cell. The optimal microstructures with required macroscopic properties, including prescribed effective properties (Sigmund 1994), extreme mechanical and thermal properties (Sigmund and Torquato 1997), and maximum structural stiffness (Neves et al. 2000; Fujii et al. 2001) have already been found for periodical composites. Besides, the microstructural optimization formulation is also the basis of the concurrent optimization formulation of material and structures (Rodrigues et al. 2002; Coelho et al. 2008, 2009; Liu et al. 2008; Niu et al. 2009).

Among the aforementioned work, the inverse homogenization method proposed by Sigmund (1994) has become the most popular method till now. The homogenization method that is based on periodicity assumption and asymptotic expansion technique is originally used to predict the macroscopic properties of heterogeneous materials (Bensoussan et al. 1978; Guedes and Kikuchi 1990) and to design structures on the macro level (Bendsøe and Kikuchi 1988). Recently, Zhang et al. (2007) offered an alternative method, based on the equivalence of strain energy and addressed that the results agreed well with those from the inverse homogenization method.

W. Su · S. Liu (✉)
State Key Laboratory of Structural Analysis for Industrial Equipment,
Department of Engineering Mechanics, Dalian University
of Technology, Dalian 116024, China
e-mail: stliu@dlut.edu.cn

W. Su
School of Civil and safety Engineering, Dalian Jiaotong University,
Dalian 116028, China
e-mail: wenzhengsu@gmail.com

It should be pointed out that the above two mentioned methods are both based on the classical continuum mechanics theory. This theory lacks any intrinsic length scales, and hence, effectively presents just a first-order approximation to a number of problems with microstructures (Jasiuk and Ostoja-Starzewski 1995). The above fact implies that the referred methods are valid only if the micro-structure's size is much smaller than that of the macro-structure or, more precisely, than the wavelength of the mechanical loading. In other words, remarkable size effect is observed when the macroscopic dimension of specimen becomes close to the order of the micro-structural length scale. For example, in the analysis of periodic multilayered cellular solid beams, the flexural rigidity cannot be obtained correctly by the classical homogenization method when the number of the plies is small. However, the size effect decreased rapidly as the increase of the microstructures (Burgueno et al. 2005; Dai and Zhang 2008).

There are usually two approaches to deal with this type of size effects. One way is to explicitly model the discrete microstructures morphology that is referred to as the direct method. This discrete model agrees well with the experiments results; however, is very costly due to computational expense for complex micro-structures. The other method, the generalized continuum method, is to homogenize or smear the heterogeneity of cellular material and to replace the cellular material by some generalized continuum, such as micropolar continuum or couple-stress continuum (Mindlin 1963; Anderson and Lakes 1994; Fleck et al. 1994). The micropolar type theory, first proposed by brothers Cosserat at 1909, further developed by Mindlin (1963), Toupin (1964) etc., was finally extended to the micropolar theory by Eringen (1966, 1999). The couple-stress theory is more preferable since it is currently considered as the simplest form of micropolar theory, and is more accurate with size effect of cellular materials (Tekoglu 2007; Tekoglu and Onck 2008).

Similar to the analysis, the optimization procedure also contains the size effect. The fundamental feature of the size effect of the microstructural optimization is that the optimal topology changes as the size ratio of macrostructure to microstructure changes (Zhang and Sun 2006). In short, the optimal topology is size-dependent. There are also two ways to simulate the size effect, i.e. the direct method and the generalized continuum method. Though size effect may have great influence on the topology design solution, not many studies have been done so far. Bendsøe and Triantafyllidis (1990) studied the elastic buckling design in terms of cell size. Zhang and Sun (2006) investigated the size effect on the optimal configuration of core material microstructure in the rigidity optimization of sandwich structures. In these

two researches, the microstructures are explicitly modeled morphology while the analytical solution and the variable linking technique are performed, respectively, to decrease the computational expense. For complicated structures, this direct method will be more time consuming compared to general continuum model, and makes the latter more suitable for these structures. However, seeking the optimal topology based on the generalized continuum model is a total recent subject. Rovati and Veber (2007) discussed the optimal topologies of micropolar solids; but it is just on the macroscopic level. Owing to the success on the research of size effect in cellular materials (Tekoglu 2007; Tekoglu and Onck 2008), we discuss the size effect in the optimization of microstructures of cellular material in terms of the couple-stress theory in this paper.

Although capable of grasping the information of microstructures, the couple-stress continuum model faces two main challenges going into wide application. The first one is the constitutive constants are exceptionally hard to measure by experiments (Lakes 1986). Fortunately, for periodic heterogeneous composite materials, an alternative way to obtain these parameters is through the analysis of the microstructures of a base cell. It has been shown that some kinds of materials, such as the cellular materials, the lattice materials and, the multi-phase composites can all be homogenized as couple-stress continuum (Bouyge et al. 2001; Bigoni and Drugan 2007; Tekoglu 2007; Tekoglu and Onck 2008). The other challenge lies in the FE analysis. In fact, C_1 continuity of element is required in the FE construction of couple-stress theory (Soh and Chen 2004; Zheng et al. 2004). Compared with the classical elasticity theory, the couple-stress theory is more complicated and, the FE method is still the most useful technique for the implementation of the theory. It is a popular topic for computational mechanics researchers to construct effective FE formulations on couple-stress theory all along.

In this paper, we propose an optimization formulation for the optimal layout of periodic material unit cell, based on the couple-stress theory. The formulation can simulate the size effect emerged during the optimization procedure since the couple-stress theory contains high order information of material microstructures. An equivalent strain energy based RVE method is established to derive the effect couple-stress constitutive constants, by the analysis of a base cell with designed boundary conditions. The SIMP power law is adopted to relate the densities, i.e. the design variables and the element stiffness matrix of RVE. The numerical examples we got indicate that our method is superior to the conventional one in the size-dependent microstructure design.

2 Introduction to couple-stress theory

The remarkable feature of the Cosserat theory lies in the fact that each point has six degrees of freedom of a rigid body, i.e. it is made of interconnected material particles. Each particle is capable of displacements and rotations, which are, in general, independent functions of position and time. Couple-stress theory, also called reduced-Cosserat theory (Toupin 1964) or Cosserat pseudo-continuum theory (Nowacki 1986), is the simplest special case of Cosserat theory. In couple-stress theory, the rotations are not independent but, rather, fully described by the displacements vectors. Taking the planar problem with displacement with $\mathbf{u} = [u, v, 0]^T$ and $\boldsymbol{\phi} = [0, 0, \phi]^T$ as an example, the relationship (1) should be satisfied.

$$\phi = (\partial v / \partial x - \partial u / \partial y) / 2 \tag{1}$$

Consequently, the strain components ϵ_x , ϵ_y and γ_{xy} , as well as the curvature components κ_{xz} and κ_{yz} are defined as follows.

$$\begin{aligned} \epsilon_x &= \partial u / \partial x, & \epsilon_y &= \partial v / \partial y, & \gamma_{xy} &= \partial u / \partial y + \partial v / \partial x \\ \kappa_{xz} &= \partial \phi / \partial x, & \kappa_{yz} &= \partial \phi / \partial y, \end{aligned} \tag{2}$$

Two equations of compatibility of curvatures and strains should be satisfied.

$$\begin{cases} \kappa_{xz} = \frac{1}{2} \frac{\partial \gamma_{xy}}{\partial x} - \frac{\partial \epsilon_x}{\partial y} \\ \kappa_{yz} = \frac{\partial \epsilon_y}{\partial x} - \frac{1}{2} \frac{\partial \gamma_{xy}}{\partial y} \end{cases} \tag{3}$$

From (1~3), one may find that the second order derivatives of displacements exist in the total potential functional of a structure. That indicates that the FE formulation of couple-stress continuum requires C_1 continuity of elements. In Appendix 1, we show some FE formulation to overcome this difficulty.

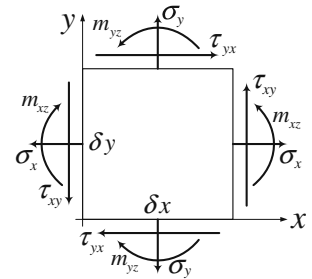
The force field is specified by the stress tensors (which is a symmetric tensor in classical elasticity but is asymmetric here) and couple-stress tensor (or moment per unit area). The stress tensor has four components as in σ_x , σ_y , τ_{xy} , τ_{yx} , and the couple-stress tensor has two components as in m_{xz} , m_{yz} (Fig. 1).

Ignoring body forces and body moments, the equations of equilibrium are given as

$$\begin{aligned} \partial \sigma_x / \partial x + \partial \tau_{yx} / \partial y &= 0, & \partial \tau_{xy} / \partial x + \partial \sigma_y / \partial y &= 0 \\ \partial m_{xz} / \partial x + \partial m_{yz} / \partial y + \tau_{xy} - \tau_{yx} &= 0 \end{aligned} \tag{4}$$

(4) implies that shear stress τ_{xy} need not be equal to τ_{yx} in couple-stress theory. Mindlin (1963) suggested resolving

Fig. 1 Rectangular components of stress and couple-stress



τ_{xy} and τ_{yx} into a symmetric part τ_S and an anti-symmetric part τ_A .

$$\tau_S = (\tau_{xy} + \tau_{yx}) / 2, \quad \tau_A = (\tau_{xy} - \tau_{yx}) / 2 \tag{5}$$

The symmetric part of the stress produces the usual shear strain while the anti-symmetric part tends to produce a local rigid rotation. Thus, the constitutive equation can be expressed as follows.

$$\begin{aligned} [\sigma_x, \sigma_y, \tau_S, m_{xz}, m_{yz}]^T \\ = \begin{bmatrix} \mathbf{C} & \mathbf{F} \\ \mathbf{F}^T & \mathbf{D} \end{bmatrix} [\epsilon_x, \epsilon_y, \gamma_{xy}, \kappa_{xz}, \kappa_{yz}]^T \end{aligned} \tag{6}$$

where, the stiffness matrix \mathbf{C} is the same as that of the classical material and matrix \mathbf{D} denotes the bending stiffness of couple-stress continuum. Especially, for the orthotropic material, the coupling term \mathbf{F} vanishes. For simplicity, the uniform periodic cell structures considered here are centrally symmetric and hence, the component of the coupling term \mathbf{F} is identically zero. Thus, the constitutive equations can be expressed in the following form.

$$\begin{aligned} \begin{Bmatrix} \sigma_x \\ \sigma_y \\ \tau_S \end{Bmatrix} &= \begin{bmatrix} C_{11} & C_{12} & 0 \\ C_{12} & C_{22} & 0 \\ 0 & 0 & C_{66} \end{bmatrix} \begin{Bmatrix} \epsilon_x \\ \epsilon_y \\ \gamma_{xy} \end{Bmatrix}, \\ \begin{Bmatrix} m_{xz} \\ m_{yz} \end{Bmatrix} &= \begin{bmatrix} D_{11} & 0 \\ 0 & D_{22} \end{bmatrix} \begin{Bmatrix} \kappa_{xz} \\ \kappa_{yz} \end{Bmatrix} \end{aligned} \tag{7}$$

3 Procedure of topology optimization

The purpose of this paper is to find the layout of material in the micro-domain that minimizes the mean compliance (or maximizes the global stiffness) of the macrostructure, subject to the constraint of the permitted material volume fraction, within a unit cell of microstructures (Fig. 2). In other words, we want to design microstructural topologies

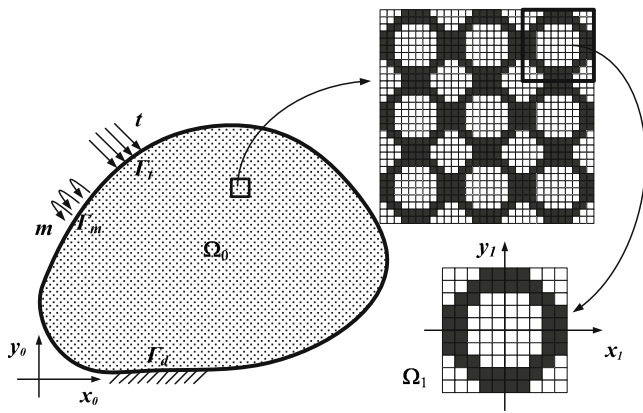


Fig. 2 Sketch of a structure with material microstructure

that give us some desirable overall properties. In order to reveal the size effect in the optimization procedure, the heterogeneous material with periodic microstructures is homogenized as couple-stress continuum with effective macroscopic properties by the RVE method. On the micro-level, the SIMP law is used to relate the design variables with the FE stiffness. Without loss of generality, the researched model is assumed to be in a state of plane stress.

Thus the optimization problem can be established as:

$$\begin{aligned}
 &\text{find } \boldsymbol{\rho} = [\rho_1, \rho_2, \dots, \rho_n]^T \\
 &\min_{\{C^H, D^H\}} l(\tilde{\mathbf{u}}) \\
 &\text{s.t. } :a(\tilde{\mathbf{u}}, \tilde{\mathbf{v}}) = l(\tilde{\mathbf{v}}) \\
 &g(\boldsymbol{\rho}) = \sum_{e=1}^n \int_{\Omega_1^e} \rho_e d\Omega_1 - V^* \leq 0 \\
 &0 < \rho_{\min} \leq \rho_e \leq 1, e = 1, \dots, n
 \end{aligned} \tag{8}$$

where the energy bilinear form $a(\tilde{\mathbf{u}}, \tilde{\mathbf{v}})$ and the load linear form $l(\tilde{\mathbf{u}})$ are defined as

$$\begin{aligned}
 a(\tilde{\mathbf{u}}, \tilde{\mathbf{v}}) &= \int_{\Omega_0} \left[\boldsymbol{\varepsilon}^T(\tilde{\mathbf{u}}) \mathbf{C}^H(\boldsymbol{\rho}) \boldsymbol{\varepsilon}(\tilde{\mathbf{v}}) \right. \\
 &\quad \left. + \boldsymbol{\kappa}^T(\tilde{\mathbf{u}}) \mathbf{D}^H(\boldsymbol{\rho}) \boldsymbol{\kappa}(\tilde{\mathbf{v}}) \right] d\Omega_0 \\
 l(\tilde{\mathbf{u}}) &= \int_{\Gamma_t + \Gamma_m} \tilde{\mathbf{t}}^T \tilde{\mathbf{u}} dS
 \end{aligned} \tag{9}$$

in which $\boldsymbol{\rho}$ denotes the design variables, i.e. the “densities”, V^* denotes the permitted material volume fractions, the superscript “ H ” denotes the effective properties of the heterogeneous material, $\tilde{\mathbf{u}}$ denotes the generalized displacement vector (including the transition and the rotation degrees of freedom), $\tilde{\mathbf{t}}$ denotes the generalized surface traction vector (including the traction force and the traction moment), $\tilde{\mathbf{v}}$ is the arbitrary generalized virtual displacement

vector, Ω_0 denotes the macroscopic domain while Ω_1 denotes the microscopic domain.

$$\boldsymbol{\varepsilon} = [\varepsilon_x, \varepsilon_y, \gamma_{xy}]^T, \boldsymbol{\kappa} = [\kappa_{xz}, \kappa_{yz}]^T, \tilde{\mathbf{u}} = [u, v, \phi]^T \tag{10}$$

It should be noted that the body force and body moment are ignored in (9).

The flowchart of present optimization procedure is shown as Fig. 3. The two key points of this problem are the determination of the effective couple-stress constitutive constants C^H and D^H as well as the sensitivity analysis.

3.1 Effective couple-stress model of heterogeneous materials

This section discusses the determination of the effective couple-stress continuum constitutive constants from the RVE of the designing material. In fact, this issue has been shown by the authors (Liu and Su 2009) before. To make this paper self-contained, we will repeat the proposition briefly. Since the considered materials are of periodic repetitions of a basic cell, only one basic cell is taken as the RVE. We consider different boundary conditions for determination of the different components of the constitutive constants for a RVE domain Ω_1 with the boundary $\partial\Omega_1$. For simplicity sake, the thickness in z -axis is set to 1 in all cases. In each case we force the unit cell to bear the designed specific deformation with $[\varepsilon_x, \varepsilon_y, \gamma_{xy}, \kappa_{xz}, \kappa_{yz}]^T$, and compute, with the FE method, the total elastic strain energy U_{disc} stored in the unit cell with the corresponding boundary conditions. The strain energy U_{cont} stored in the effective homogeneous couple-stress continuum can be obtained by the prescribed strain/stress fields. Thus the

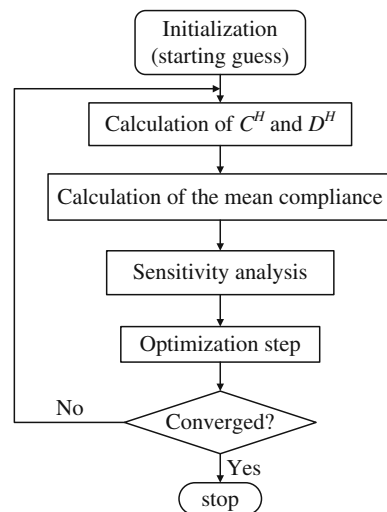


Fig. 3 Flowchart of the optimization procedure

components of the effective constitutive constants can be produced through $U_{disc} = U_{cont}$.

To determine the components of stiffness matrix C^H , we conduct the following four tests.

Test 1 (Horizontal uniaxial extension test for C_{11}^H): by applying the unit strain to the unit cell

$$\varepsilon_x = 1, \quad \varepsilon_y = \gamma_{xy} = 0, \quad \kappa_{xz} = \kappa_{yz} = 0, \quad \text{in } \Omega_1 \quad (11)$$

The corresponding boundary conditions are

$$u = x, \quad v = 0, \quad \text{on } \partial\Omega_1 \quad (12)$$

Then it follows that

$$C_{11}^H = 2U_{disc}^{(1)} / V \quad (13)$$

where V is the volume of the RVE.

Test 2 (Vertical uniaxial extension test for C_{22}^H): by applying the unit strain to the unit cell

$$\varepsilon_x = \gamma_{xy} = 0, \quad \varepsilon_y = 1, \quad \kappa_{xz} = \kappa_{yz} = 0, \quad \text{in } \Omega_1 \quad (14)$$

The corresponding boundary conditions are

$$u = 0, \quad v = y, \quad \text{on } \partial\Omega_1 \quad (15)$$

Then it follows that

$$C_{22}^H = 2U_{disc}^{(2)} / V \quad (16)$$

Test 3 (Biaxial extension test for C_{12}^H): by applying the unit strain to the RVE

$$\varepsilon_x = \varepsilon_y = 1, \quad \gamma_{xy} = 0, \quad \kappa_{xz} = \kappa_{yz} = 0, \quad \text{in } \Omega_1 \quad (17)$$

The corresponding boundary conditions are

$$u = x, \quad v = y, \quad \text{on } \partial\Omega_1 \quad (18)$$

which follows that

$$C_{12}^H = \left(2U_{disc}^{(3)} / V - C_{11}^H - C_{22}^H \right) / 2 \quad (19)$$

Test 4 (Shearing test for C_{66}^H): by applying the unit strain to the RVE

$$\varepsilon_x = \varepsilon_y = 0, \quad \gamma_{xy} = 1, \quad \kappa_{xz} = \kappa_{yz} = 0, \quad \text{in } \Omega_1 \quad (20)$$

The corresponding boundary conditions are

$$u = y/2, \quad v = x/2, \quad \text{on } \partial\Omega_1 \quad (21)$$

It yields that

$$C_{66}^H = 2U_{disc}^{(4)} / V \quad (22)$$

To determine the components of stiffness matrix D^H , we need to conduct the following two bending tests.

Test 5 (Bending test for D_{11}^H): by applying the prescribed strain/stress

$$\varepsilon_x = -y, \quad \sigma_y = 0, \quad \gamma_{xy} = 0, \quad \kappa_{xz} = 1, \quad \kappa_{yz} = 0, \quad \text{in } \Omega_1 \quad (23)$$

The corresponding boundary conditions are

$$u \Big|_{\partial\Omega_1} = -xy, \quad v \Big|_{y=0} = x^2 / 2 \quad (24)$$

It follows that

$$D_{11}^H = 2 \left(U_{disc}^{(5)} - \int_{\Omega_1} \frac{1}{2} E_x^H \cdot y^2 dV \right) / V \quad (25)$$

Test 6 (Bending test for D_{22}^H): by applying the prescribed strain/stress

$$\sigma_y = 0, \quad \varepsilon_y = x, \quad \gamma_{xy} = 0, \quad \kappa_{xz} = 0, \quad \kappa_{yz} = 1, \quad \text{in } \Omega_1 \quad (26)$$

The corresponding boundary conditions are

$$u \Big|_{x=0} = -y^2 / 2, \quad v \Big|_{\partial\Omega_1} = xy \quad (27)$$

It follows that

$$D_{22}^H = 2 \left(U_{disc}^{(6)} - \int_{\Omega_1} \frac{1}{2} E_y^H \cdot x^2 dV \right) / V \quad (28)$$

It should be noted that the following relations are implied in the above derivations.

$$\begin{aligned} E_x^H &= C_{11}^H \left(1 - C_{12}^{H2} / C_{11}^H C_{22}^H \right) \\ E_y^H &= C_{22}^H \left(1 - C_{12}^{H2} / C_{11}^H C_{22}^H \right) \end{aligned} \quad (29)$$

Till now we have constructed the effective couple-stress model of heterogeneous materials. The authors have to stress that this method will sometimes slightly overestimate the effective stiffness properties since the present method is based on the analysis of RVE with prescribed displacement boundary conditions. However, the effective couple-stress material constants are accurate enough for most cases (Liu and Su 2009).

3.2 Sensitivity analysis

When solving structural optimization problems through the gradient based numerical algorithms, one usually needs to differentiate the objective function and constraint functions with respect to the design variables. The procedure to

obtain these derivatives, or sensitivities, is called sensitivity analysis. This section performs this procedure.

For most cases, the compliance of macrostructures should be computed by the FE method. Recalling (9), the compliance can be expressed in the discrete form

$$c(\rho) = \tilde{U}_0^T \mathbf{K}_0 \tilde{U}^T \tag{30}$$

where \tilde{U}_0 is the generalized nodal displacements of the macrostructure and, \mathbf{K}_0 is the macrostructural global stiffness. From the procedure of classical FE method:

$$\mathbf{K}_0 = \sum_{i=1}^m \mathbf{k}_0^i(\rho) \tag{31}$$

where \mathbf{k}_0^i has been extended to global level. If the load is design independent, the sensitivity can be shown as:

$$\frac{\partial c(\rho)}{\partial \rho_e} = -\tilde{U}_0^T \left[\sum_{i=1}^m \frac{\partial \mathbf{k}_0^i(\rho)}{\partial \rho_e} \right] \tilde{U}_0, e = 1, \dots, n \tag{32}$$

Since

$$\mathbf{k}_0^i(\rho) = \int_{\Omega_0^i} \mathbf{B}_i^T \tilde{\mathbf{D}}^H(\rho) \mathbf{B}_i d\Omega_0^i \tag{33}$$

where $\tilde{\mathbf{D}}^H$ is defined as

$$\tilde{\mathbf{D}}^H \equiv \begin{bmatrix} \mathbf{C}^H & \mathbf{B}^H \\ (\mathbf{B}^H)^T & \mathbf{D}^H \end{bmatrix} \tag{34}$$

Then the sensitivity of the objective function is finally expressed as

$$\frac{\partial c(\rho)}{\partial \rho_e} = -\tilde{U}_0^T \left[\sum_{i=1}^m \int_{\Omega_0^i} \mathbf{B}_i^T \frac{\partial \tilde{\mathbf{D}}^H(\rho)}{\partial \rho_e} \mathbf{B}_i d\Omega_0^i \right] \tilde{U}_0, e = 1, \dots, n \tag{35}$$

From Section 3.1, the components of $\tilde{\mathbf{D}}^H$ can be determined by six different loading cases. In each case, we need to calculate the strain energy stored in the RVE under the specified displacements boundary conditions. Zhang et al. (2007) have shown the derivatives of classical effective constitutive constants with respect to the design variables. To make the paper self-contained, we derive the corresponding

derivatives in the Appendix 2 in detail. Only the results are shown here as (36).

$$\begin{aligned} \frac{\partial C_{11}^H}{\partial \rho_e} &= 2pU_e^{(1)} / \rho_e V \\ \frac{\partial C_{22}^H}{\partial \rho_e} &= 2pU_e^{(2)} / \rho_e V \\ \frac{\partial C_{12}^H}{\partial \rho_e} &= 2p(U_e^{(3)} - U_e^{(1)} - U_e^{(2)}) / \rho_e V \\ \frac{\partial C_{66}^H}{\partial \rho_e} &= 2pU_e^{(4)} / \rho_e V \\ \frac{\partial C_{11}^H}{\partial \rho_e} &= 2pU_e^{(5)} / \rho_e V - \left(\frac{\partial E_x^H}{\partial \rho_e} \right) \int_{\Omega_1} y^2 dV / V \\ \frac{\partial C_{22}^H}{\partial \rho_e} &= 2pU_e^{(6)} / \rho_e V - \left(\frac{\partial E_y^H}{\partial \rho_e} \right) \int_{\Omega_1} x^2 dV / V \end{aligned} \tag{36}$$

where $U_e^{(j)}$ denotes the strain energy stored in the eth element of the RVE under loading case j . Substituting (36) into (35), one can determine the sensitivity of the objective function to the design variables.

The sensitivity of the constraint function with respect to the design variables can be acquired straightforward (37), where A_e denotes the area or volume of the element corresponding to the eth design variable.

$$\frac{\partial g(\rho)}{\partial \rho_e} = \int_{\Omega_1^e} d\Omega_1 = A_e; e = 1, \dots, n \tag{37}$$

4 Examples and results

Two typical numerical examples are presented to demonstrate the proposed optimization formulation within the context of two-dimensional structures. The chosen base solid material is aluminum alloy with Young’s modulus $E = 69 \text{ GPa}$, Poisson’s ratio $\nu = 0.33$. Each unit cell is assumed to be central-symmetrical, thus only 1/4 of the unit cell is investigated. In order to reveal the size effect in the optimization procedure, we discuss the optimal couple-stress based topologies of unit cell of different size as well as the classical results.

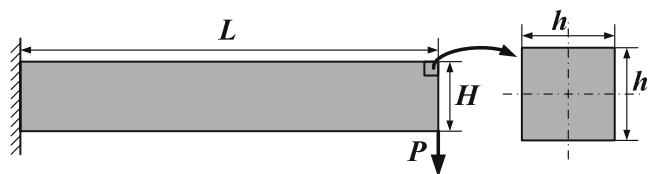
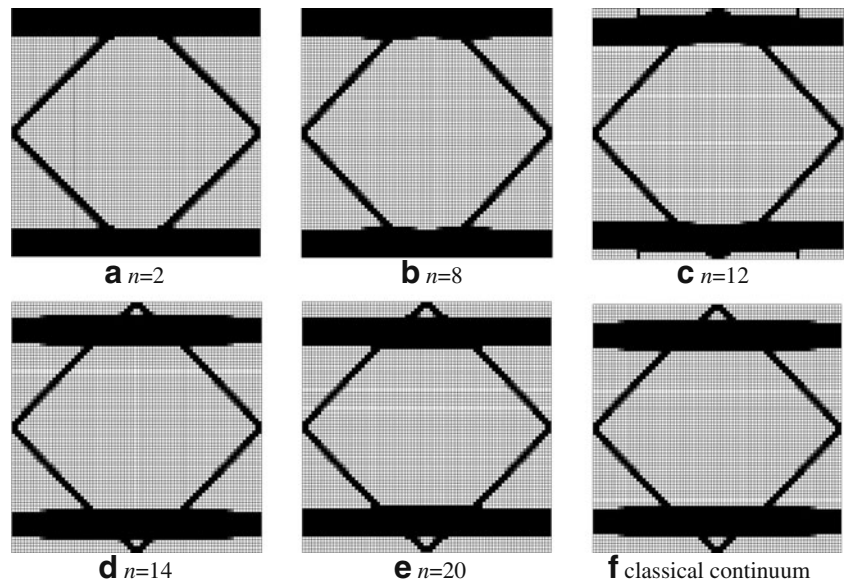


Fig. 4 Sketch of cantilever beam with design domain

Fig. 5 The optimal microstructures of the cantilever beam



4.1 Example 1: periodic cellular cantilever beam design

Consider a periodic cellular multilayered cantilever beam with length $L = 600$ mm, height $H = 100$ mm, and thickness 1. The beam is subject to a central force $P = 100$ kN on the right-lower corner (Fig. 4).

Since the macrostructure is a beam, we use the analytic solution to get the structural compliance. It may be expressed in the form of (38). Consequently, the sensitivity can be analytically solved by substituting the (36) into (38).

$$c = P \left(\frac{PL^3}{2D} + k \frac{PL}{GA} \right) \tag{38}$$

where D denotes the flexural rigidity of couple-stress beam (in Appendix 3, we show a brief derivation of this parameter), $G (= C_{66}^H)$ denotes the effective shear modulus of cellular material, k denotes the shearing factors of beams and, usually $0.8 \leq k \leq 1.2$, in this example we set $k = 1$. The second term in the bracket of (38) represents the beam’s shearing deflection while it is neglected in the case of slender beams.

In the optimization procedure, we fix the structural size of the beam and change the size of the unit cell to seek the optimal topologies of the microstructures. The index $n (= H/h)$ is used to describe the size ratio of the macrostructure to microstructure. In this case, n also denotes the layer number of the periodic beam physically.

From Fig. 5, as n (i.e. the ratio of beam height to length scale of the unit cell) increases, the optimal topology of the microstructure, based on the couple-stress continuum model, changes consequently. These findings indicate that the couple-stress continuum model can express the size effect during the optimization procedure which cannot be simulated by the classical continuum model. In detail, when

n is small, the size of macrostructure and that of microstructure are in the same order, which makes the couple-stress effect significant. Under that effect, the material tends to stay on the boundaries of the unit cell design domain to increase the bending-resistance properties. As n increases, the couple-stress effect weakens gradually and when n is large enough, the couple-stress effect can be ignored, in which case, the couple-stress continuum turns into a classical continuum. Therefore, the couple-stress based optimal topology is nearly the same as that of the classical model.

The size effect is also exhibited from the compliance of the structure (Fig. 6). In the classical model, the compliance keeps unchanged as n increases. However, the corresponding results from the couple-stress model increases sharply as n increases. In reality, due to the size decrease of the unit cell, the design space of the macrostructure is reduced so that the objective function increases and converges to the classical results. The couple-stress continuum model

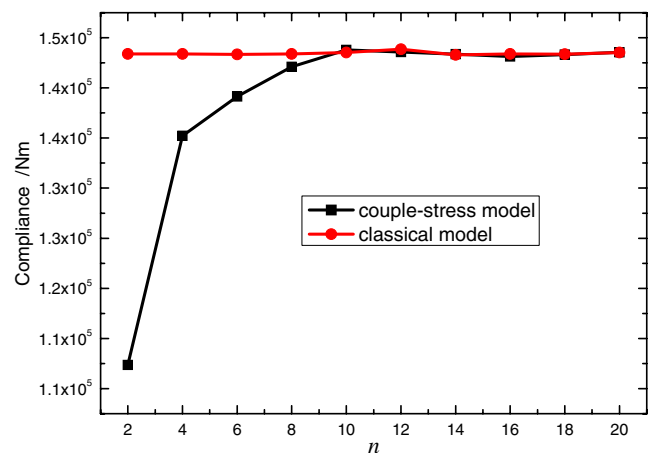


Fig. 6 The optimal objective against the ply number

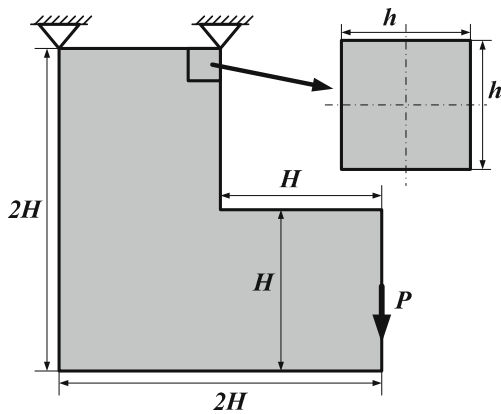


Fig. 7 Sketch of the L-beam and the design unit cell domain

can grasp this tendency which cannot be expressed by the classical continuum model.

It should be noted that the obtained results appear to be similar to those reported earlier by Zhang and Sun (2006). The difference is that they obtained the results by explicitly modeling the microstructures morphology while we obtained our results by the effective continuum model.

4.2 Example 2: periodic cellular L-beam design

Consider an L-beam with $H = 100$ mm, bearing a central shearing force $P = 50$ kN at the right end (Fig. 7). The thickness of the L-beam is set to be 1. The optimal microstructures with different length h are sought. The length ratio $n = H/h$ is also defined to relate the macro-size with the micro-one.

The FE method is used to get the structural compliance since it is hard to get an analytical solution for this problem.

We present a four-node discrete couple-stress quadrilateral element formulation in Appendix 1. Besides the material volume constraint, two additional constraint functions (39) are imported in this example. We will give a detailed explanation in the next section.

$$D_{11}^H \geq 0; D_{22}^H \geq 0 \quad (39)$$

The couple-stress based optimal topology depends remarkably on the size ratio n (Fig. 8). Similar features are observed as n changes to what observed in Example 1.

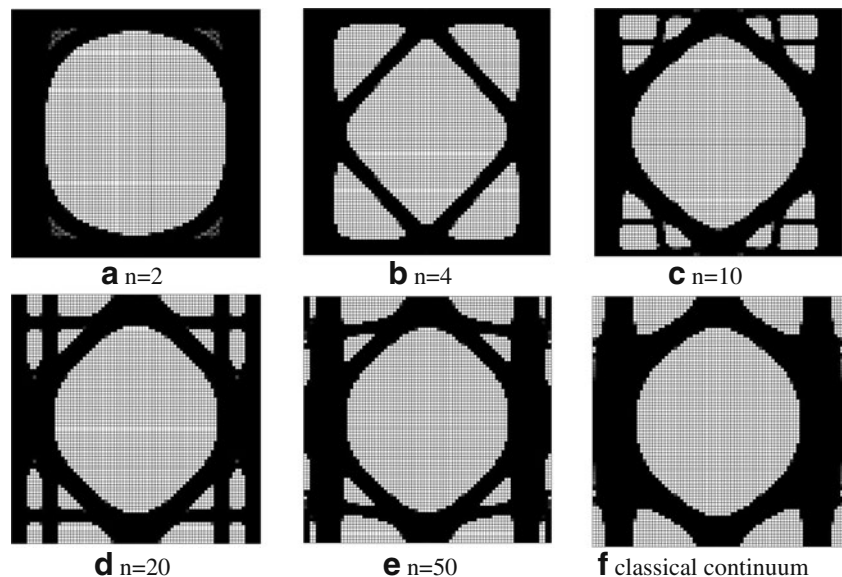
The same tendency is observed from the evolution of the objective function against the increase of the ratio (Fig. 9). Different from the classical result, the couple-stressed based result increases sharply and eventually converges to the classical result as the length scale of the unit cell decreases. When the size of macrostructures is far larger than that of the microstructures, the couple-stress continuum turns into the classical continuum.

4.3 Discussions

Similar to the classical optimization model, the checkerboard pattern is observed in the present couple-stress based optimization formulation. One can eliminate this numerical instability by the filtering technique (Bruns and Tortorelli 2001; Sigmund 2007). Besides, there are two more aspects that should pay attention to.

First, the present method has some dependency on the initial guess, especially when the size of microstructure is far smaller than that of the macrostructure. In short, the initial homogeneous distribution of densities will lead to iteration infeasibility in these cases. This phenomenon can be interpreted from the sensitivity of the objective function.

Fig. 8 Optimal microstructures of the L-beam



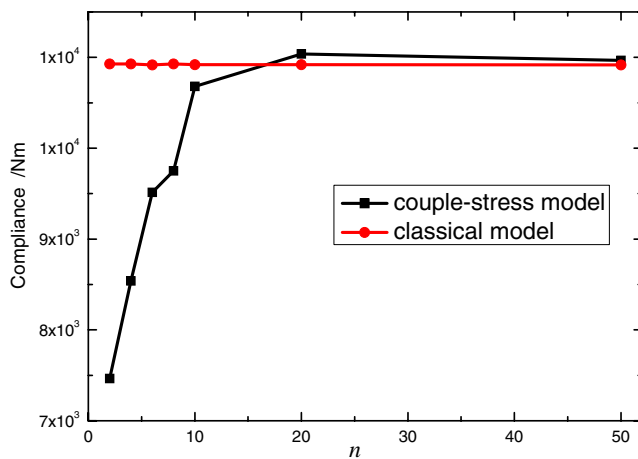


Fig. 9 The optimal objective against the ply number

The key point of the sensitivity analysis is the sensitivity of the effective constitutive constants with respect to design variables. From (36), initial homogeneous distribution of design variables means the homogeneous distribution of $\partial C/\partial \rho_e$. Thus for the classical model, this homogeneous distribution of derivatives will also lead to the homogeneous distribution of the sensitivity of the objective function. On the other hand, for couple-stress model, when the ratio is small, the couple-stress effect is significant, thus the sensitivity distribution is not homogeneous since the $\partial \mathbf{D}/\partial \rho_e$ is not homogeneous. However, if the ratio is large enough, the couple-stress effect is small enough to be ignored; thus the sensitivity distribution is approximately to be homogeneous. Hence, the iteration will be infeasible.

The second problem is that the additional constraints (39) are necessary if the macrostructural compliance has to be computed through the FE method. Bigoni and Drugan (2007) have pointed out that the composites can not be homogenized to couple-stress continuum unless the inclusion phase is softer than the matrix phase (for example, the solid base material with a void). Otherwise, the bending moduli will no longer be positive. In other words, the permitted material lies in the center of the design domain will lead to the negative bending modulus \mathbf{D} . Since the FE method is mostly based on the variational principle that requires the positive definite of the constitutive matrix, the constraints (39) have to be satisfied. However, the import of the inequality (39) confines the feasible set of the initial structural optimization problem, thus the result may not strictly converge to the optimal solution sometimes. For example, in the optimization of the L-beam, when the ratio is large enough, the couple-stress based result is close yet not equal to the classical result, and the objective function is slightly bigger than the classical results. Fortunately, when the ratio is large enough, the couple-stress effect can

be totally ignored, thus one can model it by the classical method.

5 Conclusion

In this paper, we introduced the concept of couple-stress into the microstructure design of periodic material. This new model can grasp the size effect lying in the optimization procedure since the couple-stress theory contains high order information of microstructure.

We should remark that the present results can also be realized through the fully discretization model with the variable linking technique. To some extent, this discrete model is even more accurate since it contains the complete features of microstructures. But our method has two significant advantages. First, the present method is of greater computational efficiency due to the use of the effective continuum model. Although it seems we need six loading cases to determine the effective couple-stress continuum constants, the global stiffness in the FE analysis of these loading cases are exactly the same, which makes the whole procedure simple and efficient. Second, our model is more convenient to integrate into the concurrent optimization model of material and structures since the structural mesh and the material mesh are completely uncoupling.

Compared with the classical method, the present method has remarkable advantages. However, the present approach is limited to the periodic microstructures with central-symmetry only. For the microstructures without symmetry, we need additional work to determine the coupling constitutive constants \mathbf{F} , which is difficult. A more general method is currently under investigation.

Acknowledgments The authors are thankful for valuable discussions on finite element formulation with Professor Changliang Zheng of Dalian maritime university and grateful to Miss Jiaqi Liu of Oxford University for her kind help with the language and writing style of this paper. The author WS also thanks Professor Jamie Guest of Johns Hopkins University for his valuable comments. The present work was supported by the National Natural Science Foundation of China through the Grant No. (90816025, 90605002 and 10721062), National Basic Research Program of China (2006CB601205), and SRFDP (200801411052). The authors gratefully acknowledge these financial supports.

Appendix 1: Formulation of discrete couple-stress quadrilateral element

FE analysis is a restricting factor against the application of couple-stress theory since the theory requires the C_1 continuity of displacements. In this section, we derive a four-node quadrilateral FE formulation, based on the technique of discrete couple-stress constraint (Zheng et al. 2004), to

implement the optimization procedure. The total potential functional (without body force and body moment) is

$$\Pi = \int_{\Omega_0} \frac{1}{2} (\boldsymbol{\varepsilon}^T \mathbf{C} \boldsymbol{\varepsilon} + \boldsymbol{\kappa}^T \mathbf{D} \boldsymbol{\kappa}) d\Omega_0 - \int_{\Gamma_i + \Gamma_m} \tilde{\mathbf{t}}^T \tilde{\mathbf{u}} dS \quad (40)$$

The displacement vector of element is discretized as (41)

$$\tilde{\mathbf{u}} = \mathbf{N} \tilde{\mathbf{d}}_e \quad (41)$$

where \mathbf{N} is the shape function matrix of generalized displacement which would be explained in the following context and $\tilde{\mathbf{d}}_e$ is the generalized nodal displacement vector.

The corresponding geometry equations are

$$\begin{aligned} \boldsymbol{\varepsilon} &= \mathbf{L}_u \tilde{\mathbf{u}} = \mathbf{L}_u \mathbf{N} \tilde{\mathbf{d}}_e = \mathbf{B}_u \tilde{\mathbf{d}}_e, \\ \boldsymbol{\kappa} &= \mathbf{L}_\phi \tilde{\mathbf{u}} = \mathbf{L}_\phi \mathbf{N} \tilde{\mathbf{d}}_e = \mathbf{B}_\phi \tilde{\mathbf{d}}_e \end{aligned} \quad (42)$$

Hence the total potential functional of an element is

$$\begin{aligned} \Pi^e &= \int_{\Omega_0^e} \frac{1}{2} (\tilde{\mathbf{d}}_e^T \mathbf{B}_u^T \mathbf{C} \mathbf{B}_u \tilde{\mathbf{d}}_e + \tilde{\mathbf{d}}_e^T \mathbf{B}_\phi^T \mathbf{D} \mathbf{B}_\phi \tilde{\mathbf{d}}_e) d\Omega_0^e \\ &\quad - \int_{\Gamma_i^e + \Gamma_m^e} \tilde{\mathbf{d}}_e^T \mathbf{N}^T \tilde{\mathbf{t}} dS^e \end{aligned} \quad (43)$$

The element stiffness matrix, obtained from the variation of (43), is superposed by two terms as

$$\mathbf{K}^e = \mathbf{K}_u^e + \mathbf{K}_\phi^e = \int_{\Omega_0^e} \mathbf{B}_u^T \mathbf{C} \mathbf{B}_u d\Omega_0^e + \int_{\Omega_0^e} \mathbf{B}_\phi^T \mathbf{D} \mathbf{B}_\phi d\Omega_0^e \quad (44)$$

where the former term is the conventional element stiffness matrix, based on the classical elasticity theory and generalized to global level; the latter one is the special term of the couple-stress continuum. We proceed to derive the second term in the natural coordinate.

The interpolation functions of the generalized displacement are

$$u = \sum_{i=1}^4 N_i u_i, \quad v = \sum_{i=1}^4 N_i v_i, \quad \phi = \sum_{i=1}^4 N_i \phi_i + \alpha N_\alpha \quad (45)$$

Where, N_i is the four-node Lagrange interpolates function (Zienkiewicz et al. 2005); N_α is a bubble function (46), and α is an undetermined coefficient, ξ and η denotes the natural coordinates.

$$N_\alpha = (1 - \xi^2)(1 - \eta^2)/8 \quad (46)$$

Thus the macro-rotation of each point in an element can be described as

$$\omega_z = \frac{1}{2} \left[\sum_{i=1}^4 (\partial N_i / \partial x) v_i - \sum_{i=1}^4 (\partial N_i / \partial y) u_i \right] \quad (47)$$

We force the macro-rotation to equal the micro-rotation on the given constraint point ($\xi = \eta = 0$), i.e.

$$\begin{aligned} \frac{1}{2} \left[\sum_{i=1}^4 (\partial N_i / \partial x) v_i - \sum_{i=1}^4 (\partial N_i / \partial y) u_i \right] \\ = \sum_{i=1}^4 N_i \phi_i + \alpha N_\alpha \end{aligned} \quad (48)$$

The value of α can be determined by (48). Substituting α into (45) and (42) sequentially, we find the expression of \mathbf{B}_ϕ and, finally, we obtain the element stiffness formulation \mathbf{K}^e . In brief, the requirement of C_1 continuity is relaxed by the discrete couple-stress constraint technique.

Appendix 2: Sensitivity of \mathbf{C}^H and \mathbf{D}^H

This appendix derives all the derivatives of the effective couple-stress constitutive constants with respect to the design variables which are necessary for the structural compliance sensitivity (35). The derivatives can be found directly from the procedure of the computation of \mathbf{C}^H and \mathbf{D}^H .

Consider the RVE, which has been discretized into n finite elements and, each element is assigned by a density variable ρ_e ($e = 1, \dots, n$). Following the SIMP assumption, the element stiffness matrix is related to the density variable in the power form.

$$\mathbf{k}_1^i = \rho_i^p \tilde{\mathbf{k}}_1^i, \quad i = 1, \dots, n \quad (49)$$

where $\tilde{\mathbf{k}}_1^e$ denotes the element stiffness matrix made of solid material, p the penalty factor and $p > 1$. From Section 3.1, the determination of different components of \mathbf{C}^H and \mathbf{D}^H needs six loading cases. In each loading case, we need to perform an FE analysis to compute the strain energy under the specified displacement boundary conditions. Thus the FE governing equation can be expressed as

$$\mathbf{K}_1 \mathbf{U}_1^{(j)} = \mathbf{P}_1^{(j)}, \quad j = 1, \dots, 6 \quad (50)$$

where \mathbf{K}_1 denotes the global structural stiffness of the RVE, and $\mathbf{U}_1^{(j)}$ and $\mathbf{P}_1^{(j)}$ the nodal displacements and load vector in loading case j respectively. Extend \mathbf{k}_1^e to the global level, then

$$\mathbf{K}_1 = \sum_{e=1}^n \rho_e^p \tilde{\mathbf{k}}_1^e \quad (51)$$

The sensitivity of the strain energy of the RVE with respect to the element density variable ρ_e can be expressed as

$$\begin{aligned} \frac{\partial U_{disc}^{(j)}}{\partial \rho_e} &= \frac{1}{2} \frac{\partial}{\partial \rho_e} \left[\mathbf{U}_1^{T(j)} \mathbf{K}_1 \mathbf{U}_1^{(j)} \right] \\ &= \frac{1}{2} \left[2 \frac{\partial \mathbf{U}_1^{T(j)}}{\partial \rho_e} \mathbf{P}_1^{(j)} + \mathbf{U}_1^{T(j)} \frac{\partial \mathbf{K}_1}{\partial \rho_e} \mathbf{U}_1^{(j)} \right] \\ e &= 1, \dots, n; j = 1, \dots, 6 \end{aligned} \tag{52}$$

It should be noted that the equilibrium (50) of the RVE can be rewritten in the following form

$$\begin{bmatrix} \mathbf{K}_1^{ii} & \mathbf{K}_1^{io} \\ \mathbf{K}_1^{oi} & \mathbf{K}_1^{oo} \end{bmatrix} \begin{Bmatrix} \mathbf{U}_1^{i(j)} \\ \mathbf{U}_1^{o(j)} \end{Bmatrix} = \begin{Bmatrix} \mathbf{P}_1^{i(j)} \\ \mathbf{P}_1^{o(j)} \end{Bmatrix}, \tag{53}$$

where the superscript ‘‘o’’ denotes the nodes on which the prescribed displacements are imposed. The superscript ‘‘i’’ denotes the rest nodes. Following important information is implied in equation

$$\mathbf{P}_1^{i(j)} = \mathbf{0}, \frac{\partial \mathbf{U}_1^{o(j)}}{\partial \rho_e} = \mathbf{0}; \quad e = 1, \dots, n; j = 1, \dots, 6 \tag{54}$$

Substituting (54) into (52), one will find

$$\begin{aligned} \frac{\partial U_{disc}^{(j)}}{\partial \rho_e} &= \frac{1}{2} \left[2 \left(\frac{\partial \mathbf{U}_1^{i(j)T}}{\partial \rho_e} \mathbf{0} \right) \begin{Bmatrix} \mathbf{0} \\ \mathbf{P}_1^{o(j)} \end{Bmatrix} + \mathbf{U}_1^{T(j)} \frac{\partial \mathbf{K}_1}{\partial \rho_e} \mathbf{U}_1^{(j)} \right] \\ &= \frac{1}{2} \mathbf{U}_1^{T(j)} \frac{\partial \mathbf{K}_1}{\partial \rho_e} \mathbf{U}_1^{(j)} = \frac{p}{\rho_e} \mathbf{u}_e^{(j)} \\ e &= 1, \dots, n; j = 1, \dots, 6 \end{aligned} \tag{55}$$

From (55), one can obtain the results of (36). Since the strain energy has been computed, no additional FE analysis is required for the sensitivity analysis.

Appendix 3: Flexural rigidity of couple-stress continuum beam

Consider a straight beam made of couple-stress continuum with height H and thickness b , which subject to the pure bending load (Fig. 10). Taking moment equilibrium in the cross section of the beam, following equation is derived.

$$M = - \int_A y \sigma_x dA + \int_A m_{xz} dA \tag{56}$$

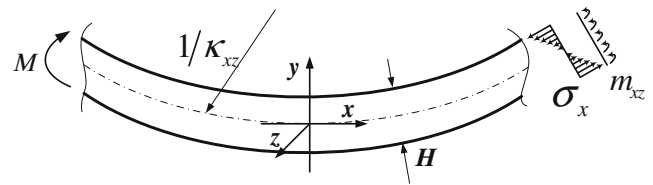


Fig. 10 Sketch of a couple-stress continuum beam

If the plane assumption for the deformation of cross-section is used, then

$$\sigma_x = -E_x y \kappa_{xz} + \sigma_x |_{y=0} \tag{57}$$

(56) becomes

$$M = (E_x I_z + D_{11} A) \kappa_{xz} \tag{58}$$

where $I_z (= \int_A y^2 dA = bH^3/12$, for rectangular cross-section) and A are the moment of inertia and area, respectively, of the beam’s cross section. Thus the flexural rigidity of the couple-stress continuum beam D is defined as

$$D = E_x I_z + D_{11} A \tag{59}$$

It has the same form as micropolar continuum beam (Huang et al. 2000), where the first term denotes the flexural rigidity of classical continuum while the second term denotes the modification term of couple-stress continuum beams.

References

Anderson WB, Lakes RS (1994) Size effects due to Cosserat elasticity and surface damage in closed-cell polymethacrylimide foam. *J Mater Sci* 29:6413–6419

Bendsøe MP (1989) Optimal shape design as a material distribution problem. *Struct Multidisc Optim* 1:193–202

Bendsøe MP, Kikuchi N (1988) Generating optimal topologies in structural design using a homogenization method. *Comput Methods Appl Mech Eng* 71:197–224

Bendsøe MP, Sigmund O (2004) *Topology optimization: theory, methods and applications*. Springer, Berlin

Bendsøe MP, Triantafyllidis N (1990) Scale effects in the optimal design of a microstructured medium against buckling. *Int J Solids Struct* 26:725–741

Bensoussan A, Lions J-L, Papanicolaou G (1978) *Asymptotic analysis for periodic structures*. Elsevier, Amsterdam

Bigoni D, Drugan WJ (2007) Analytical derivation of Cosserat moduli via homogenization of heterogeneous elastic materials. *J Appl Mech* 74:741–753

Bouyge F, Jasiuk I, Ostoja-Starzewski M (2001) A micromechanically based couple-stress model of an elastic two-phase composite. *Int J Solids Struct* 38:1721–1735

Bruns TE, Tortorelli DA (2001) Topology optimization of non-linear elastic structures and compliant mechanisms. *Comput Methods Appl Mech Eng* 190:3443–3459

- Burgueno R, Quagliata MJ, Mohanty AK et al (2005) Hierarchical cellular designs for load-bearing biocomposite beams and plates. *Mater Sci Eng A* 390:178–187
- Coelho P, Fernandes P, Guedes J et al (2008) A hierarchical model for concurrent material and topology optimisation of three-dimensional structures. *Struct Multidisc Optim* 35:107–115
- Coelho PG, Fernandes PR, Rodrigues HC et al (2009) Numerical modeling of bone tissue adaptation—a hierarchical approach for bone apparent density and trabecular structure. *J Biomech* 42:830–837
- Dai GM, Zhang WH (2008) Size effects of basic cell in static analysis of sandwich beams. *Int J Solids Struct* 45:2512–2533
- Eringen AC (1966) Linear theory of micropolar elasticity. *J Math Mech* 15:909–923
- Eringen AC (1999) *Microcontinuum field theories*, vol 1. Springer, New York
- Fleck NA, Muller GM, Ashby MF et al (1994) Strain gradient plasticity: theory and experiment. *Acta Metall Mater* 42:475–487
- Fujii D, Chen BC, Kikuchi N (2001) Composite material design of two-dimensional structures using the homogenization design method. *Int J Numer Methods Eng* 50:2031–2051
- Guedes J, Kikuchi N (1990) Preprocessing and postprocessing for materials based on the homogenization method with adaptive finite element methods. *Comput Methods Appl Mech Eng* 83:143–198
- Huang F-Y, Yan B-H, Yan J-L et al (2000) Bending analysis of micropolar elastic beam using a 3-D finite element method. *Int J Eng Sci* 38:275–286
- Jasiuk I, Ostoja-Starzewski M (1995) Planar Cosserat elasticity of materials with holes and intrusions. *Appl Mech Rev* 48:11–18
- Lakes RS (1986) Experimental microelasticity of two porous solids. *Int J Solids Struct* 22:55–63
- Liu S, Su W (2009) Effective couple-stress continuum model of cellular solids and size effects analysis. *Int J Solids Struct* 46:2787–2799
- Liu L, Yan J, Cheng G (2008) Optimum structure with homogeneous optimum truss-like material. *Comput Struct* 86:1417–1425
- Mindlin RD (1963) Influence of couple-stresses on stress concentrations. *Exp Mech* 3:1–7
- Neves MM, Rodrigues H, Guedes JM (2000) Optimal design of periodic linear elastic microstructures. *Comput Struct* 76:421–429
- Niu B, Yan J, Cheng G (2009) Optimum structure with homogeneous optimum cellular material for maximum fundamental frequency. *Struct Multidisc Optim* 39:115–132
- Nowacki W (1986) *Theory of asymmetric elasticity*. Pergamon, Oxford
- Rodrigues H, Guedes JM, Bendsoe MP (2002) Hierarchical optimization of material and structure. *Struct Multidisc Optim* 24:1–10
- Rovati M, Veber D (2007) Optimal topologies for micropolar solids. *Struct Multidisc Optim* 33:47–59
- Sigmund O (1994) Materials with prescribed constitutive parameters: an inverse homogenization problem. *Int J Solids Struct* 31:2313–2329
- Sigmund O (2007) Morphology-based black and white filters for topology optimization. *Struct Multidisc Optim* 33:401–424
- Sigmund O, Torquato S (1997) Design of materials with extreme thermal expansion using a three-phase topology optimization method. *J Mech Phys Solids* 45:1037–1067
- Soh A-K, Chen W (2004) Finite element formulations of strain gradient theory for microstructures and the C^{0-1} patch test. *Int J Numer Methods Eng* 61:433–454
- Tekoglu C (2007) Size effects in cellular solids. University of Groningen, Groningen
- Tekoglu C, Onck PR (2008) Size effects in two-dimensional Voronoi foams: a comparison between generalized continua and discrete models. *J Mech Phys Solids* 56:3541–3564
- Toupin RA (1964) Theories of elasticity with couple-stress. *Arch Ration Mech Anal* 17:85–112
- Zhang W, Sun S (2006) Scale-related topology optimization of cellular materials and structures. *Int J Numer Methods Eng* 68:993–1011
- Zhang W, Dai G, Wang F et al (2007) Topology optimization of material microstructures using strain energy-based prediction of effective elastic properties. *Acta Mech Sin* 23:73–89
- Zheng C-I, Ren M-f, Zhang Z-f et al (2004) Analysis of elastic Cosserat medium using discrete Cosserat finite elements. *Chinese J Comput Phys* 21:377–382
- Zienkiewicz OC, Taylor RL, Zhu JZ (2005) *The finite element method: its basis and fundamentals*. Elsevier, Oxford